Planta (2014) 239:847–863
DOI 10.1007/s00425-013-2018-6

ORIGINAL ARTICLE

Accumulation of acidic SK_3 dehydrins in phloem cells of cold- and drought-stressed plants of the Solanaceae

Bartosz Mieczyslaw Szabala · Sylwia Fudali · Tadeusz Rorat

Received: 4 October 2013 / Accepted: 20 December 2013 / Published online: 7 January 2014

Abstract The role of acidic SK_n dehydrins in stress tolerance of important crop and model species of the Solanaceae remains unknown. We have previously shown that the acidic SK_3 dehydrin DHN24 from *Solanum sogarandinum* is constitutively expressed and its expression is associated with cold acclimation. Here we found that DHN24 is specifically localized to phloem cells of vegetative organs of non-acclimated plants. More precise localization of DHN24 revealed that it is primarily found in sieve elements (SEs) and companion cells (CCs) of roots and stems. In cold-acclimated plants, DHN24 is mainly present in all cell types of the phloem. *Dhn24* transcripts are also predominantly localized to phloem cells of cold-acclimated stems. Immunoelectron microscopy localized DHN24 to the cytosol and close to organelle membranes of phloem cells, the lumen with phloem protein filaments, parietal cytoplasm of SEs and the nucleoplasm of some nuclei. Cell fractionation experiments revealed that DHN24 was detected in the cytosolic, nuclear and microsomal fractions. We also determined whether homologous members of the acidic subclass dehydrins from *Capsicum annuum* and *Lycopersicon chilense* share the characteristics of DHN24. We showed that they are also constitutively expressed, but their protein level is upregulated preferentially by drought stress. Immunofluorescent localization revealed that they are detected in SEs and CCs of unstressed plants and throughout the phloem in drought-stressed plants. These results suggest that one of the primary roles of DHN24 and its homologs may be the protection of the phloem region from adverse effects of abiotic stresses.

Keywords Abiotic stress · Cell fractionation · Dehydrin · Immunolocalization · Phloem · Solanaceae

Abbreviations
CC Companion cell
SE Sieve element

Introduction

Dehydrative environmental conditions trigger a wide array of plant responses including changes in gene expression, accumulation of osmoprotectants and synthesis of hydrophilic proteins such as dehydrins (Bartels and Sunkar 2005; Mahajan and Tuteja 2005). Dehydrins generally accumulate to high levels during seed maturation and in vegetative tissues in response to low temperature, drought, or high salinity. Their increased accumulation is linked to the acquisition of tolerance to a variety of dehydrative stresses (Hanin et al. 2011). Dehydrins are characterized by a highly conserved lysine-rich amino acid domain (EKKGIMDKIKEKLPG), named the K-segment, that is present in one or several copies near the C-terminus. The K-segment is found in all dehydrins and believed to play

B. M. Szabala · T. Rorat
Institute of Plant Genetics, Polish Academy of Sciences, Strzeszynska 34, 60-479 Poznan, Poland

Present Address:
B. M. Szabala (✉)
Department of Plant Genetics, Breeding and Biotechnology, Faculty of Horticulture and Landscape Architecture, Warsaw University of Life Sciences, SGGW, Nowoursynowska St 159, 02-776 Warsaw, Poland
e-mail: bartszab@poczta.fm; bartosz_szabala@sggw.pl

S. Fudali
Department of Botany, Faculty of Agriculture and Biology, Warsaw University of Life Sciences, SGGW, Nowoursynowska St 159, 02-776 Warsaw, Poland

a role in protein–lipid interactions (Close 1997). Other domains found in dehydrins include a tract of phoshorylable serine residues (the S-segment), a consensus sequence DEYGNP (the-Y-segment) located near the N-terminus and a less conserved region rich in polar amino acids (the Φ-segment). Based on the presence of highly conserved segments, different subclasses of dehydrins have been proposed: Y_nSK_n, SK_n, K_n, Y_nK_n, K_nS (Close 1997). Many dehydrins are found in the cytosol and nucleus (Goday et al. 1994; Houde et al. 1995; Egerton-Warburton et al. 1997). Some of them are also present in different cell compartments such as mitochondria (Borovskii et al. 2000), outer surface of plasma membrane (Danyluk et al. 1998), or vacuoles (Heyen et al. 2002).

Although their physiological functions are not completely understood, dehydrins are postulated to preserve the integrity of macromolecules and cellular structures under severe conditions of dehydration stress. In vitro experiments have demonstrated that many dehydrins have cryoprotective activity towards sensitive enzymes (Hara 2010). Koag et al. (2003) have showed that DHN1 binds anionic phospholipid vesicles, and the binding is mediated by the presence of the K-segments (Koag et al. 2009). Other putative functions of dehydrins include nucleic acid (Hara et al. 2009) and metal (Svensson et al. 2000) binding, radical scavenging (Hara et al. 2004, 2013) and protection of membrane lipid against peroxidation (Hara et al. 2003).

Acidic dehydrins of SK_n type constitute another subclass of the dehydrin family, first distinguished by Danyluk et al. (1994). These dehydrins generally accumulate in plant cells in response to low temperature and appear to be involved in the development of freezing tolerance (Rorat 2006). Acidic SK_n dehydrins have been shown to bind anionic phospholipids, calcium ions in a phosphorylation-dependent manner and protect labile enzymes from thermal-induced denaturation (Alsheikh et al. 2005; Kovacs et al. 2008). They are also present at substantial levels under normal growth conditions (Robertson and Chandler 1994; Nylander et al. 2001), showing tissue-specific distribution, which suggests some specialized role during plant growth. In cold-acclimated *Arabidopsis* plants, acidic dehydrins can be found in most cells (Nylander et al. 2001), whereas in cold-acclimated wheat they exhibit more specific localization (Danyluk et al. 1998).

In Solanaceous species, which comprise important crop and model plants, acidic SK_n dehydrins have not been characterized at the tissue and cellular levels and, therefore, no data are available about their potential roles under optimal and stress conditions. In our previous work, we have isolated and characterized a cold-induced gene from *Solanum sogarandinum* encoding the 24-kDa acidic SK_3 dehydrin DHN24 (Rorat et al. 2006). We have found that DHN24 is constitutively present in plant organs and its expression is associated with cold acclimation. To improve the knowledge of DHN24 function under low-temperature stress and during normal growth, we undertook a comprehensive study to identify the tissues and cells that accumulate DHN24 and determine its precise subcellular localization. We also investigated the accumulation of DHN24 homologs from *Capsicum annuum* and *Lycopersicon chilense* at the protein, tissue and cellular levels to further characterize the members of this subclass of dehydrins in the Solanaceae.

Materials and methods

Plant material and growth conditions

Solanum sogarandinum (Ohoa, PI 230510), *Lycopersicon chilense,* LA1930 (Tomato Genetics Resource Center TGRC, Davis, USA), *Capsicum annuum* (Sweet pepper), cv Roberta (Warsaw University of Life Sciences, SGGW) plants were grown in a climate chamber at 20/18 °C (day/night) under a 14-h photoperiod with a light intensity of 200 μmol m^{-2} s^{-1}. Cold treatment was performed by transferring 2- to 3-week-old plants to a temperature of 5 °C for 7 days. Drought stress was imposed on plants by withholding watering for 14 days. For salt treatment, plants were watered twice a day with a 80 ml solution containing 250 mM NaCl for 5 days.

Preparation of antiserum

The antiserum raised against a partial fragment of DHN24 (Rorat et al. 2006) was affinity-purified using the Protein A IgG Purification Kit (Pierce) following the manufacturer's instruction. Preimmune serum was purified in the same way and used as a negative control in immunolocalization experiments.

Western blot analysis

Western blot analysis was performed as described previously (Rorat et al. 2006) using protein A-purified anti-DHN24 antibodies diluted 1:1,000 and secondary antibodies conjugated to alkaline phosphatase (Sigma) diluted 1:40,000. Soluble plant proteins were extracted in 50 mM Tris–HCl, 2 mM EDTA, pH 7.5 and 1 mM PMSF.

Tissue preparation for fluorescence and electron microscopy

Tissue samples were fixed in 4 % (w/v) paraformaldehyde in MSB buffer (50 mM PIPES, 5 mM EGTA, 5 mM $MgSO_4$, pH 6.9) at room temperature for 2 h. Fixed samples

were rinsed several times with MSB buffer to remove any residual fixative and dehydrated through a graded ethanol series (supplemented with 10 mM DTT) from 10 to 100 % (v/v). Dehydrated material was embedded in methacrylate mix (Sigma-Aldrich) (80 % (v/v) butylmethacrylate, 20 % (v/v) methylmethacrylate, 0.5 % (w/v) benzoin ethyl ether, 10 mM DTT) according to Baskin et al. (1992) or in LR White resin (Sigma) as described by Dykstra and Reuss (2003). Methacrylate-embedded material was cut into 3-μm sections on a Leica RM2165 microtome, mounted on prewarmed silane-coated slides (Sigma) and used for immunofluorescent labeling. LR White-embedded material was cut into 150-nm sections on a Leica UCT ultramicrotome, collected on formvar-coated 150-mesh nickel grids and used for immunogold labeling.

Immunofluorescent labeling

For removal of methacrylate from thin sections, slides were incubated for 10 min in acetone, rehydrated in TBS (25 mM Tris–HCl, pH 7.5, 150 mM NaCl) and blocked with 5 % (w/v) non-fat dry milk in TBS for 1 h. Slides were then incubated with the primary antibody diluted 1:400 in TBS for 1 h. After 3 × 10 min washes with TBST (TBS containing 0.05 % (v/v) Tween-20), slides were incubated with secondary goat anti-rabbit antibody conjugated to Alexa Fluor 488 (Molecular Probes) diluted 1:1,000 in 2 % (w/v) BSA (bovine serum albumin) in TBS for 1 h. After 3 × 10 min washes with TBST and distilled water, slides were examined under an Olympus AX 70 PROVIS microscope equipped with U-M61002 filter set. For photographic documentation, an Olympus DP50 digital camera was used. Control experiments were conducted by replacing primary antibody with preimmune rabbit serum or by adding the pure recombinant DHN24 (1 mg ml^{-1}) to the incubation mixture containing the primary antibody.

Aniline blue staining

Following fluorescence examination, slides were stained with 0.05 % (w/v) aniline blue in 50 mM phosphate buffer, pH 7.5 to detect callose in sieve plates.

In situ hybridization

In situ hybridization was performed as described previously (Fudali et al. 2008). Digoxigenin (DIG)-labeled 300 bp sscDNA sense and antisense probes for *Dhn24* were used for detection of *Dhn24* mRNA on sections of cold-treated stems. DIG-labeled probes were detected using Fluorescent Antibody Enhancer Set (Roche). Signal was photographed as described above.

Immunogold labeling and electron microscopy

Ultrathin sections were transferred to a drop of 2 % (w/v) BSA in TBS, pH 7.5 and blocked at room temperature for 1 h. Sections were then incubated with the primary antibody diluted 1:50 in 1 % (w/v) BSA in TBS for 1 h. After 3 × 10 min washes in TBS, grids were placed on a drop of 10 nm gold-conjugated anti-rabbit IgG (Sigma) diluted 1:50 in TBS for 1 h. Following three washes with TBS and an additional two with distilled water, sections were counterstained with 2 % (w/v) uranyl acetate. Gold-labeled sections were examined under a JEOL (Tokyo, Japan) JEM 1220 transmission electron microscope. Control experiments were conducted as described for immunofluorescent labeling.

Subcellular fractionation

Mitochondria were isolated as described by Millar et al. (2007) from cold-treated stems of *S. sogarandinum* grown in the dark for 5 days before harvesting. Plant material was ground in a Waring blender for 3 × 15 s in ice-cold homogenization medium (0.4 M sucrose, 50 mM Tris–HCl, pH 8.0, 2 mM EDTA, 0.1 % (w/v) BSA and 5 mM cysteine), filtered through 3 layers of Miracloth (Calbiochem) and centrifuged twice at 3,000*g* for 10 min to remove large particles. The supernatant was centrifuged for 20 min at 18,000*g* and the resulting organelle pellet was resuspended in wash buffer (0.4 M sucrose, 50 mM Tris–HCl pH 7.5, 2 mM EDTA). The crude mitochondrial fraction was loaded onto Percoll gradients consisting of 18, 26 and 45 % (v/v) Percoll in wash buffer. The samples were centrifuged at 27,000*g* for 1 h, and pure mitochondria were collected from the 26 %/45 % interphase.

A microsomal fraction was isolated from cold-treated stems. Plant material was ground in a Waring blender for 3 × 15 s in ice-cold homogenization medium (0.4 M sucrose, 50 mM Tris–HCl, pH 8.0, 2 mM EDTA, 1 mM PMSF, 1 mM $MgCl_2$, 0.5 % PVP and 5 mM cysteine) and filtered through 3 layers of Miracloth. The homogenate was then subjected to differential centrifugation at 3,000*g* for 10 min, 25,000*g* for 20 min and 130,000*g* for 1 h. The resulting supernatant was used as a cytosolic fraction, and the 130,000*g* pellet, which was washed twice with wash buffer (50 mM Tris–HCl, 10 mM sucrose, 10 mM KCl, 0.5 mM $CaCl_2$, 1 mM $MgCl_2$, 0.5 mM $ZnSO_4$) was used as a microsomal fraction.

Intact chloroplasts were prepared from stems of cold-acclimated *S. sogarandinum* according to Van Wijk et al. (2007). Plant material was ground in a Waring blender for 2 × 10 s in ice-cold homogenization medium (0.33 M sorbitol, 50 mM Tris–HCl, pH 8.0, 2 mM EDTA, 0.5 % (w/v)

PVP-40 and 5 mM cysteine). The homogenate was filtered through 3 layers of Miracloth and centrifuged at 2,000*g* for 10 min. Crude chloroplast pellet was resuspended in wash buffer (0.33 M sorbitol, 50 mM Tris–HCl, pH 7.5, 2 mM EDTA) and loaded on a Percoll step cushion consisting of 40 and 90 % (v/v) Percoll in wash buffer. After centrifugation at 3,800*g* for 10 min, intact chloroplasts were collected from the 40/90 % percoll interface.

Nuclei were isolated from cold-treated stems of *S. sogarandinum* as described earlier (Rorat et al. 2006).

Proteins were extracted from isolated organelles in RIPA buffer (50 mM Tris–HCl, pH 8.0, 0.1 % (w/v) SDS, 1 % (v/v) Triton, 1 % (w/v) DOC, 100 mM NaCl, 1 mM EDTA, 1 mM PMSF) and subjected to Western blot analysis. The purity of isolated chloroplasts, mitochondria, nuclei and cytosol was verified by Western blot analysis using compartment marker antibodies (Agrisera, Vännäs, Sweden) directed against cytochrome b559 (chloroplasts), isocitrate dehydrogenase (mitochondria), histone H3 (nuclei) and UDP-glucose pyrophosphorylase (cytosol).

Subfractionation of mitochondria

Subfractionation of mitochondria was performed according to Millar et al. (2007) with slight modifications. Isolated mitochondria were resuspended in ice-cold low-osmotic buffer (80 mM sucrose, 25 mM Tris–HCl, pH 7.5) and incubated on ice for 15 min. After adjusting the sucrose concentration to 400 mM, and further incubation for 10 min, the suspension was centrifuged at 16,000*g* for 15 min at 4 °C. The supernatant represented the outer mitochondrial membrane (OM) and the intermembrane space (IMS) fraction. The pellet was resuspended in 25 mM Tris–HCl, 1 mM EDTA pH 7.5 and subjected to three successive cycles of freezing in liquid nitrogen and thawing at ambient temperature. The sample was centrifuged for 15 min at 16,000*g* yielding supernatant and pellet containing the matrix (MA) and inner membrane (IM) fraction, respectively.

Results

DHN24 accumulates primarily in phloem cells of non-acclimated and cold-acclimated plants

In our previous work we have shown that DHN24 is constitutively present at similar levels in both *Solanum sogarandinum* lines that are capable and incapable of cold acclimation (Rorat et al. 2006). The DHN24 protein level is upregulated in response to cold treatment only in plants able to cold acclimate. Therefore, we used *S. sogarandinum* plants capable of cold acclimation for the experiments included in this manuscript.

We investigated in detail the localization of DHN24 at the tissue level in non-acclimated and cold-acclimated plants. Polyclonal antibodies raised against a partial fragment of recombinant DHN24 (Rorat et al. 2006) were used in immunolocalization experiments. Semi-thin cross sections of various vegetative organs were incubated with the anti-DHN24 polyclonal antibodies and labeled with secondary antibody conjugated to green fluorescent dye. In non-acclimated stems, fluorescence labeling was selectively localized to some cells of the phloem (Fig. 1a). No labeling was detected in xylem, cortex (Fig. 1a) and epidermis (data not shown). The same localization pattern was observed in petioles (Fig. 1e). Green fluorescence was also observed in some cells of the phloem in non-treated roots, but was absent from all other tissues (Fig. 1c). In non-acclimated mature leaves DHN24 was detected in the external and internal phloem of minor veins, whereas epidermis, mesophyll and xylem remained unlabeled (Fig. 1i). Under cold-stress conditions, we observed an increase in the intensity of labeling in most organs and changes in cellular localization, although the pattern of the tissue localization of DHN24 was similar to that of non-acclimated plants, being mainly restricted to the phloem. The most pronounced changes were found in stems. Most phloem cells appeared labeled, and in some cells labeling occurred more intensely (Fig. 1b). In some sections, weaker labeling was also observed in xylem parenchyma cells (Fig. 1g). No signal was observed in cortex (Fig. 1b) and epidermis (data not shown). A similar pattern of localization was observed in cold-acclimated petioles (Fig. 1f). In mature and young leaves, strong fluorescent signal was found throughout the phloem tissue (Fig. 1j, k). In cold-treated roots, more phloem cells appeared labeled compared with those in unstressed-roots (Fig. 1d). Control sections of cold-acclimated stems, petioles, mature leaves and roots incubated with preimmune antibodies were devoid of labeling (Fig. 1h, l–n). Addition of pure recombinant DHN24 to the incubation mixture containing the primary antibody greatly reduced labeling (data not shown).

Localization of *Dhn24* mRNA in cold-treated stems

We further investigated the distribution of *Dhn24* mRNA by in situ hybridization. We focused our efforts on localizing the transcripts in cold-acclimated stems. In situ experiments revealed that the localization pattern of *Dhn24* mRNA was similar to that of the protein, being predominantly observed in phloem (Fig. 2a, b). Very weak labeling was also found in cortex (Fig. 2a), and in some sections weaker labeling was detected in xylem

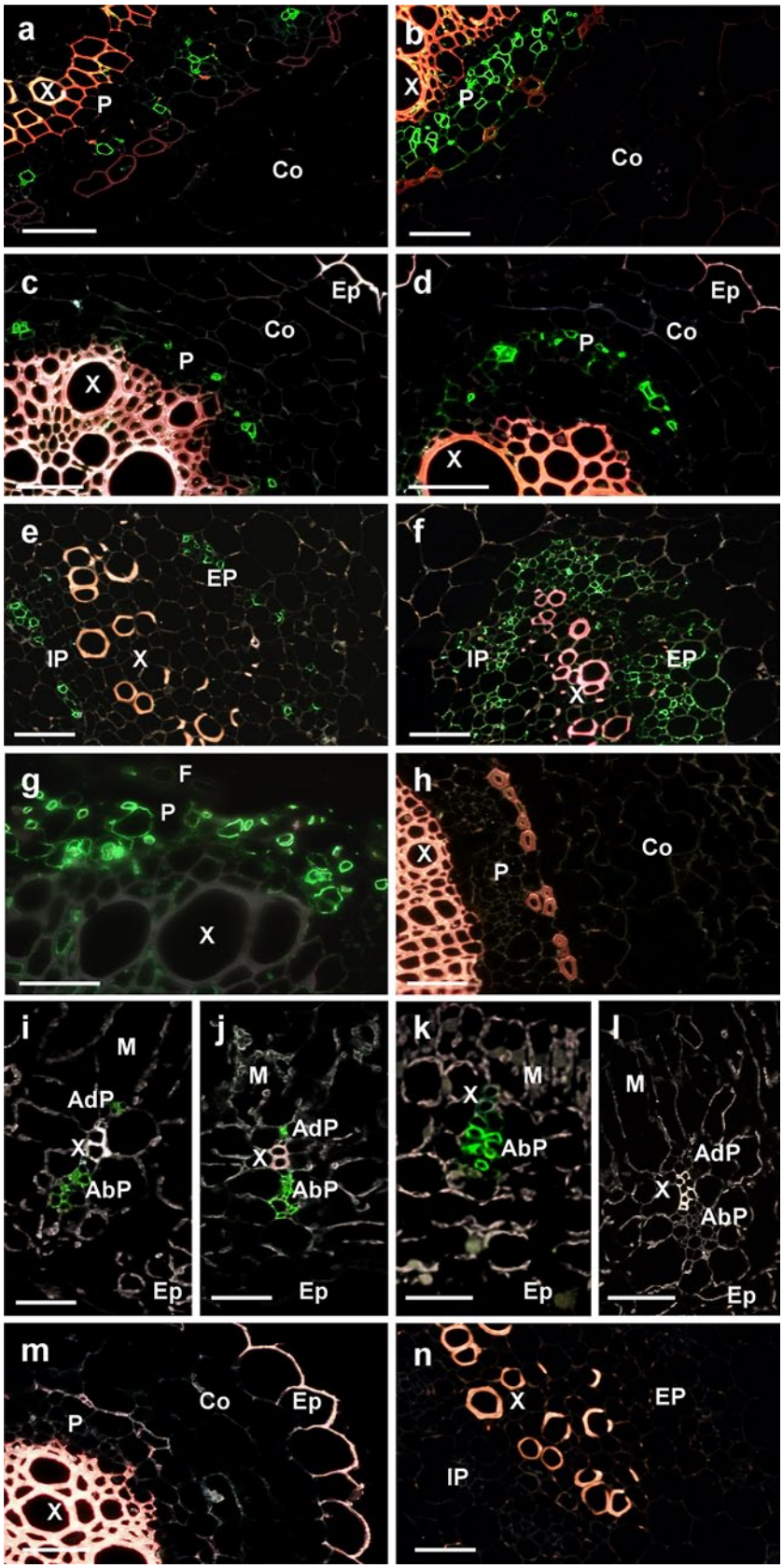

Fig. 1 Immunofluorescence localization of DHN24 in vegetative organs of *S. sogarandinum.* Cross-sections were incubated with anti-DHN24 polyclonal antibodies and labeled with secondary antibody conjugated to green fluorescent Alexa Fluor 488 dye. **a** Non-acclimated stem. **b** Cold-acclimated stem. **c** Non-acclimated root. **d** Cold-acclimated root. **e** Non-acclimated petiole. **f** Cold-acclimated petiole. **g** Cold-acclimated stem. Note the weaker labeling in xylem parenchyma cells. **i** Non-acclimated mature leaves. **j** Cold-acclimated mature leaves. **k** Cold-acclimated young leaves. Sections of cold-acclimated stems (**h**), mature leaves (**l**), roots (**m**) and petioles (**n**) treated with preimmune antibodies. *AbP* abaxial phloem, *AdP* adaxial phloem, *Co* cortex, *Ep* epidermis, *EP* external phloem, *IP* internal phloem, *M* mesophyll, *P* phloem, *X* xylem. *Bars* 25 μm

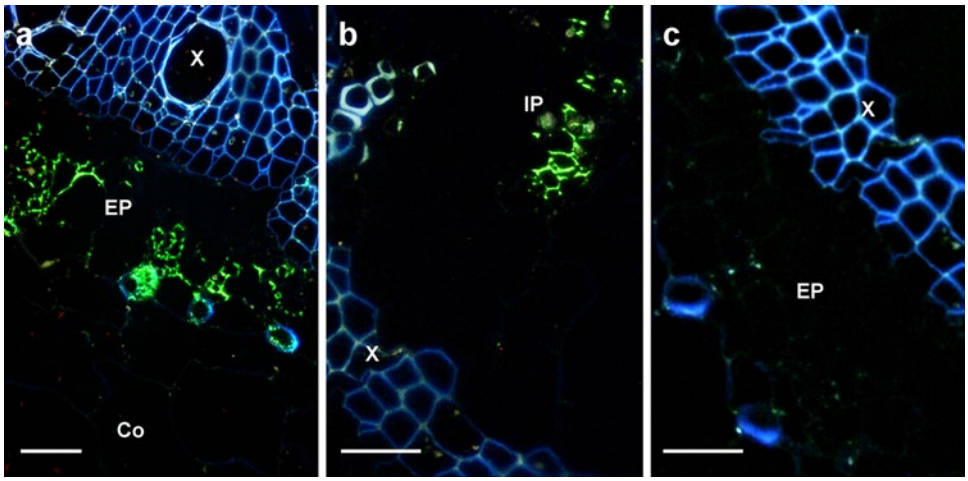

Fig. 2 Localization of *Dhn24* mRNA in cold-acclimated stems of *S. sogarandinum* by in situ hybridization. Cross-sections of stem hybridized to DIG-labeled sscDNA antisense probe (**a**, **b**) and sense probe (**c**). Hybrids were detected using fluorescent detection of DIG using antibodies conjugated to fluorescent FITC dye. *Co* cortex, *EP* external phloem, *IP* internal phloem, *X* xylem. *Bars* 25 μm

parenchyma cells (data not shown). Control experiments with *Dhn24* sscDNA sense probe gave no detectable signal (Fig. 2c).

Identification and characterization of *DHN24*-expressing cells

To identify the type of the cells in which DHN24 was localized in the phloem, we examined additional properties of the labeled cells. In transporting organs such as stems and roots of flowering plants the phloem generally consists of phloem parenchyma cells, companion cells (CCs), sieve elements (SEs) and sometimes of phloem fibers. SEs and CCs are closely associated with each other, forming the SE/CC complexes. Other typical features of SEs include the presence of callose in sieve plates and a tube-like shape, characterized by wider ends. In contrast, CCs have oval ends and are typically narrower than SEs (Van Bel et al. 2002; Van Bel 2003). Phloem fibers are easily distinguished by their tapering cells and thickened walls. Phloem parenchyma cells are found in between SE/CC complexes, rectangle-shaped and generally wider in diameter than SEs and CCs. To explore these distinctive characteristics, longitudinal sections of non-acclimated and cold-acclimated stems and roots were prepared and incubated with the anti-DHN24 polyclonal antibodies, followed by incubation with secondary antibody. Marked fluorescence was evident in SEs and CCs of non-acclimated stems (Fig. 3a, b) and roots (Fig. 3d). No detectable signal was found in phloem parenchyma and bordering cells (Fig. 3a, b, d). In cold-treated stems, most cells of the phloem were labeled including CCs, SEs, phloem parenchyma and phloem fibers (Fig. 3c). The most pronounced labeling was observed in CCs and SEs. A similar localization pattern was observed in cold-acclimated roots (Fig. 3e). The successive staining of callose in the root section from Fig. 3e using aniline blue further confirmed the presence of SEs adjoining CCs to both of which DHN24 was localized (Fig. 3f).

DHN24 has multiple locations in the cell

To examine the precise subcellular localization of DHN24, we used immunogold labeling and transmission electron microscopy (TEM). Ultrathin sections of phloem cells from cold-acclimated stems were incubated with the anti-DHN24 polyclonal antibodies and labeled with secondary antibody conjugated to colloidal gold particles. Gold particles were abundantly observed in the cytoplasm of CCs (Fig. 4b–d). Gold labeling was also observed in the nucleoplasm of some nuclei (Fig. 4c), but in lower abundance, whereas cell wall and the lumen of vacuoles did not contain signal (Fig. 4e, f). In some sections, gold particles were present close to outer mitochondrial membranes (Fig. 4e, f). In SEs, DHN24 was localized to the cytoplasm of differentiating SEs (Fig. 4i) and to the parietal cytoplasm adjoining the cell wall of mature SEs (Fig. 4j). Some DHN24 was detected in the lumen coincident with the presence of phloem protein (P-protein) filaments (Fig. 4k). Weaker labeling was also present in sieve-area pores (Fig. 4i). In control experiments, ultrathin sections incubated with pre-immune antibodies were practically absent from staining (Fig. 4g, h).

Subcellular fractionation was also performed to complement the results from TEM. Immunoblot analysis revealed that DHN24 was detected in the cytosolic, nuclear and microsomal fractions (Fig. 5a). The cytosolic fraction was most abundant in DHN24. The nuclear and microsomal fractions were free of cytosolic contamination as verified by immunoblot analysis using antibodies against the cytosolic UDP-glucose pyrophosphorylase. Chloroplastic and mitochondrial fractions did not contain detectable amounts of DHN24.

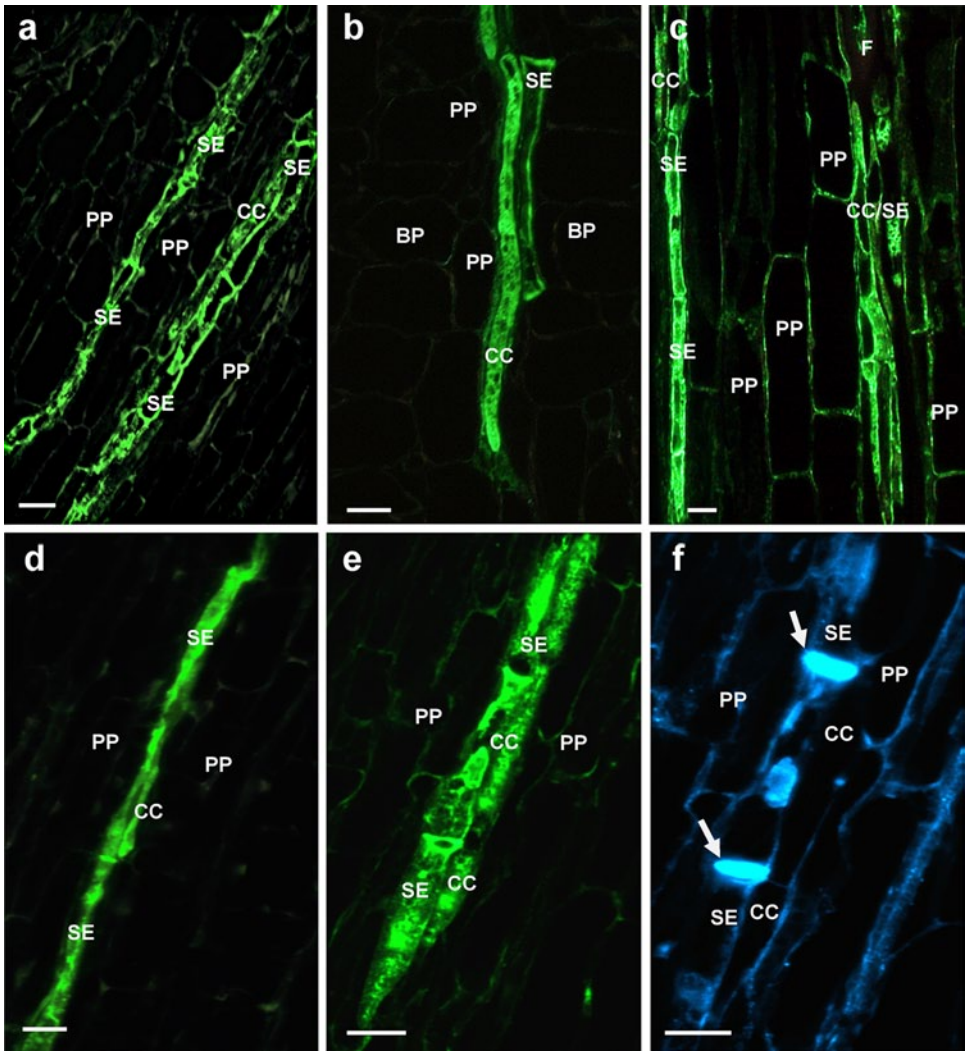

Fig. 3 Identification of the DHN24-expressing cells. Non-acclimated and cold-acclimated stem and root longitudinal sections were incubated with anti-DHN24 polyclonal antibodies and labeled with secondary antibody conjugated to green fluorescent Alexa Fluor 488 dye. Some of the labeled cells were stained with aniline blue to detect callose in sieve plates. External (**a**) and internal (**b**) phloem of non-acclimated stems. **c** Cold-acclimated stems. **d** Non-acclimated roots. Immunofluorescence localization of DHN24 in cold-acclimated roots (**e**) and successive staining of the section from **e** with aniline blue (**f**) to detect callose. *CC* companion cell, *F* phloem fiber, *PP* phloem parenchyma, *SE* sieve element. *Arrows* indicate sieve plates. *Bars* 5 μm

Considering that we observed DHN24 close to the outer mitochondrial membrane using TEM, the absence of signal in the mitochondrial fraction confirms in part results from TEM suggesting that DHN24 was not transported into mitochondria but may bind to the outer mitochondrial membrane from cytosol under certain environmental conditions. To exclude the possibility that DHN24 amounts at the outer mitochondrial membrane were too low to detect in the total mitochondrial fraction, mitochondria were fractionated into three compartments to concentrate each fraction. These comprised the outer mitochondrial membrane (OM) and intermembrane space (IMS), matrix (MA) and inner membrane (IM). After isolation of total proteins from each compartment, immunoblot analysis was performed. The positive signal for DHN24 was detected only in the OM + IMS fraction (Fig. 5b). Compartment marker antibodies directed against isocitrate dehydrogenase (mitochondrial matrix) gave the strongest signal in the MA fraction and weaker signals in the other compartments. However, antibodies against the cytosolic UDP-glucose pyrophosphorylase gave a weak positive signal in the OM + IMS fraction, which suggested that some cytosolic contamination could be present. Although the results from the biochemical fractionation approach was similar to those from TEM, we were unable to unambiguously establish whether the positive signal for DHN24 in the OM + IMS fraction was associated with its presence at the OM or with cytosolic contamination.

Accumulation, tissue distribution and cellular localization of DHN24 homologs in vegetative organs of *Lycopersicon chilense* and *Capsicum annuum* under unstressed and stressed conditions

We investigated the accumulation, tissue distribution and cellular localization of DHN24 homologs in different species of the Solanaceae family to determine whether the acidic subclass dehydrins share similar properties. The amino acid sequence of DHN24 has 84 and 89 % identity with the *Capsicum annuum* (accession no. AAO38853) and

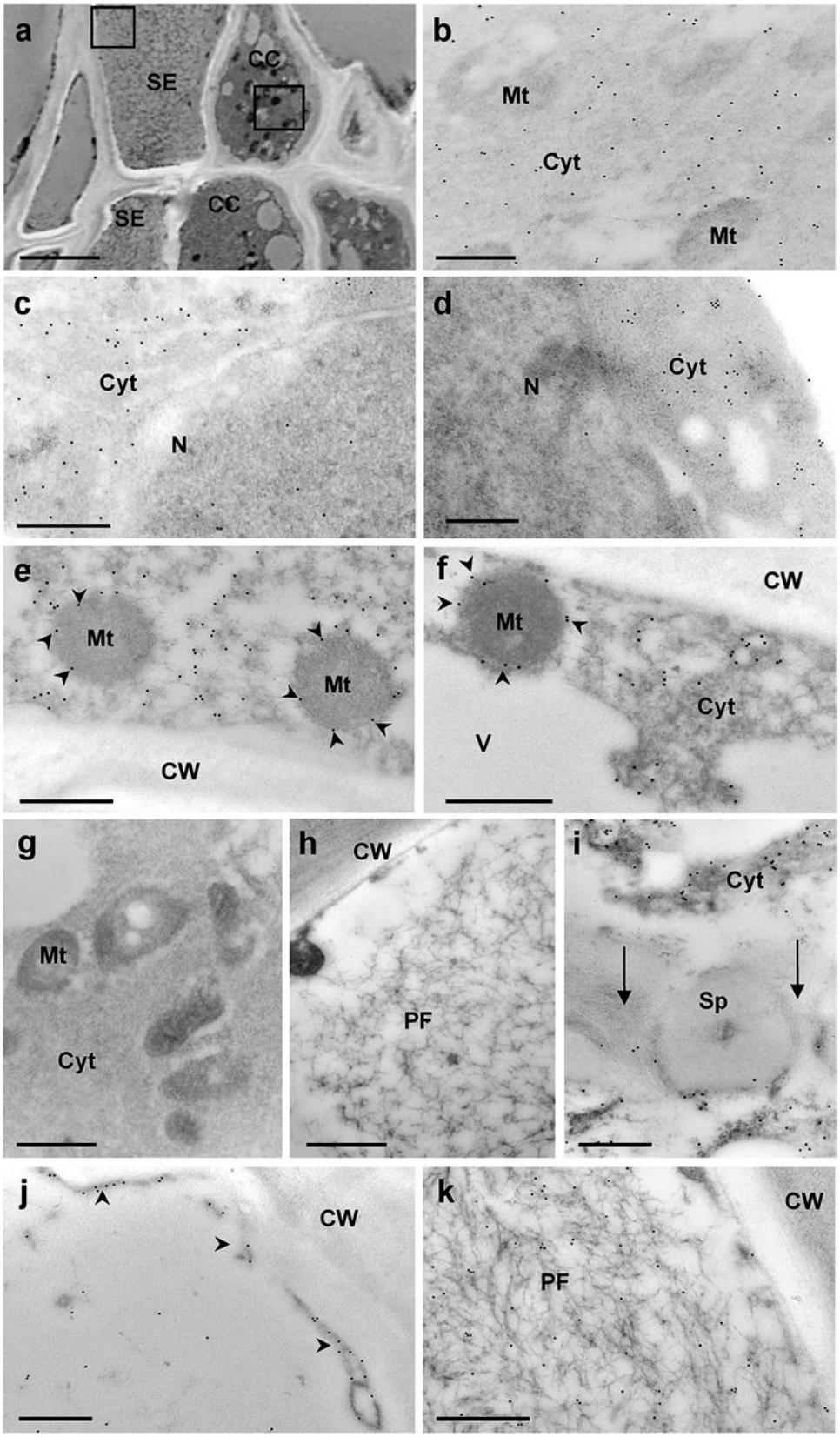

Fig. 4 Electron micrographs of cold-acclimated stem sections from *S. sogarandinum.* Ultrathin sections of the phloem tissue of cold-treated stems were incubated with anti-DHN24 polyclonal antibodies or preimmune antibodies, and labeled with secondary antibody conjugated to colloidal gold particles. **a** Phloem tissue showing the SE–CC complex. The *rectangles* in (**a**) are shown at higher magnification in (**b**) and (**k**). **b** High-magnification image of the CC from (**a**) showing localization of DHN24 to the cytosol. **c** Localization of DHN24 to the cytosol and the nucleus. **d** Cytosolic localization of DHN24. Note the weak labeling in the nucleus. **e**, **f** Fragments of CC showing labeling close to the outer mitochondrial membranes. *Arrowheads* indicate gold particles. **g**, **h** Stem sections incubated with preimmune antibodies. **i** High abundance of DHN24 in the cytosol and lower abundance in sieve-area pores of the differentiating SEs. *Arrows* indicate the location of the sieve-area pores. **j** Localization of DHN24 to the parietal cytoplasm of the mature SE. *Arrowheads* indicate gold particles. **k** High-magnification image of the SE from (**a**) showing localization of DHN24 to the SE lumen containing phloem protein (P-protein) filaments. *CC* companion cell, *Cyt* cytosol, *CW* cell wall, *Mt* mitochondrion, *N* nucleus, *PF* P-protein filaments, *PP* phloem parenchyma, *SE* sieve element, *Sp* sieve plate, *V* vacuole. *Bars* 0.5 μm (**b**–**k**), 5 μm (**a**)

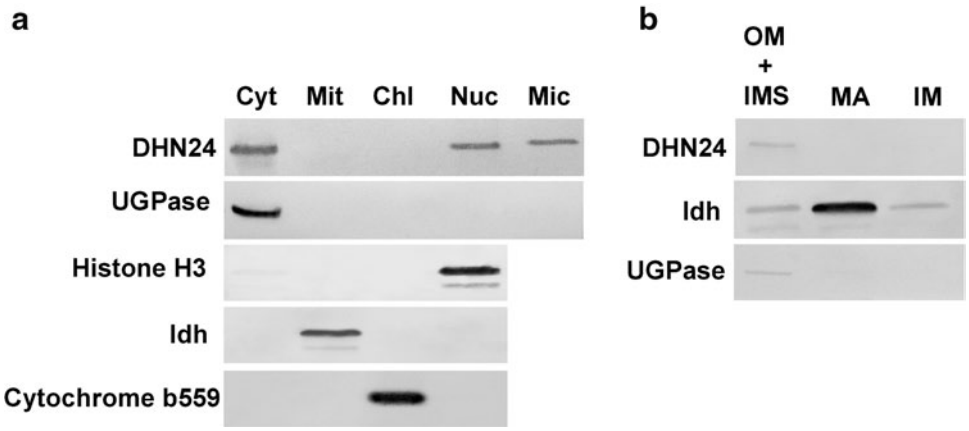

Fig. 5 Subcellular localization of DHN24. **a** Biochemical fractionation of cellular compartments. Total protein was extracted from cytosolic (Cyt), mitochondrial (Mit), chloroplastic (Chl), nuclear (Nuc) and microsomal (Mic) fractions of cold-treated stems. 15 μg of protein was loaded in each lane. DHN24 was detected by immunoblotting as described in "Materials and methods". Compartment marker antibodies (Agrisera) directed against UDP-glucose pyrophosphorylase [UGPase] (cytosol), histone H3 (nuclei), isocitrate dehydrogenase [Idh] (mitochondrial matrix) or cytochrome b559 (chloroplasts) were used in immunoblotting to confirm the purity of the isolated fractions. **b** Subfractionation of mitochondria. Mitochondria were fractionated into three compartments that comprised the outer mitochondrial membrane (OM), intermembrane space (IMS), matrix (MA) and inner membrane (IM). Total protein was extracted from each fraction and immunoblot analysis was performed using primary antibodies directed against DHN24, Idh or UGPase

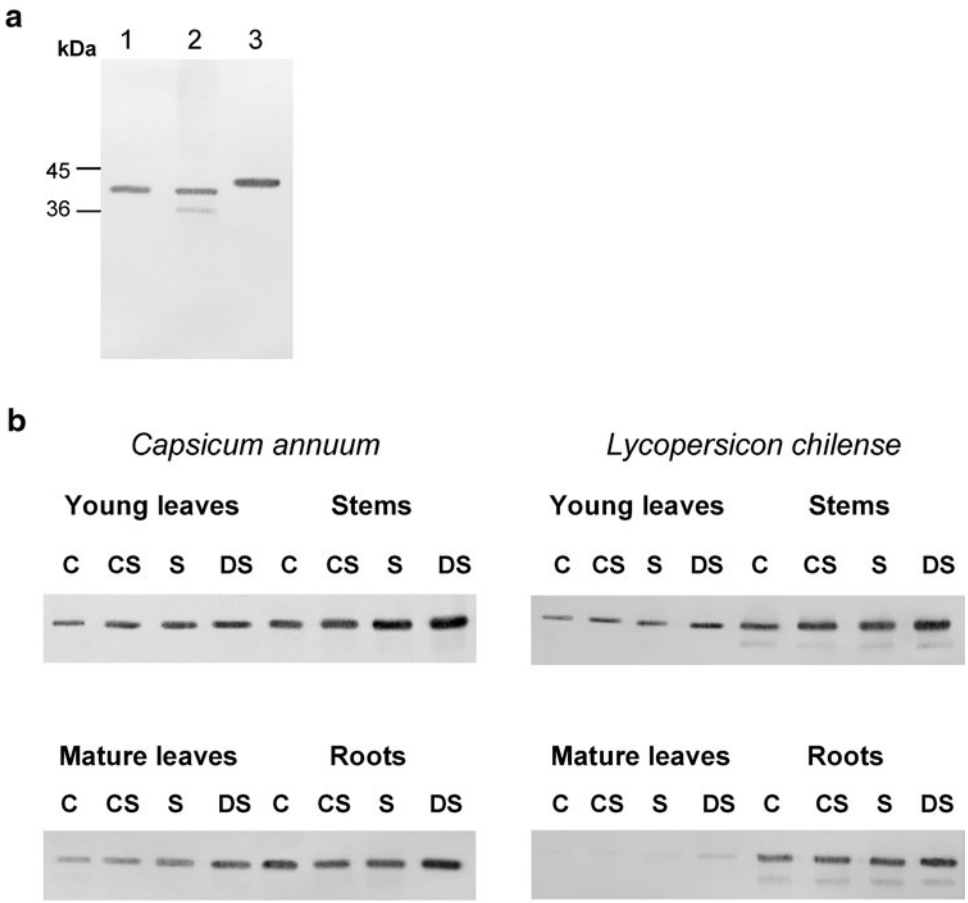

Fig. 6 Immunoblot analysis of DHN24 homologs. **a** Immunospecificity of the anti-DHN24 polyclonal antibodies. Soluble protein was extracted from non-stressed stems of *Solanum sogarandinum* (*1*), *Lycopersicon chilense* (*2*) and *Capsicum annuum* (*3*). 12 μg of protein was loaded in each lane. DHN24 and its homologs were detected by immunoblotting. **b** Accumulation of DHN24 homologs in vegetative organs of pepper (*Capsicum annuum* cv. Roberta) and wild tomato (*Lycopersicon chilense* LA1930) plants under unstressed and stressed conditions. 12 μg of protein was loaded in each lane. The proteins were separated on a 10 % SDS-PAGE gel. DHN24 homologs were detected by immunoblotting as described in "Materials and methods". *C* unstressed plants, *CS* cold stress (5 °C, 7 days), *S* salt stress (250 mM NaCl, 5 days), *DS* drought stress, (14 days after withholding watering)

Lycopersicon chilense (accession no. M97211) dehydrin homologs, respectively. For Western blot and histochemical analysis, we used *Capsicum annuum* cv Roberta and *Lycopersicon chilense* LA1930. We first determined the specificity of the anti-DHN24 polyclonal antibodies used for detection of DHN24 homologs. Immunoblot analysis showed that the antibodies recognized one protein of 43 kDa in stem extracts of pepper plants (Fig. 6a). One major protein of 41 kDa and the minor protein of 37 kDa were detected in stem extracts of wild tomato plants. The predicted masses for the *Lycopersicon* and *Capsicum* dehydrins based upon the deduced amino acid sequence are 23.2, and 24.6 kDa, respectively. The discrepancy between the calculated molecular mass and that estimated from SDS-PAGE has also been observed for DHN24 (Rorat et al. 2006; Fig. 6a) and other dehydrins (Nylander et al. 2001). The higher molecular mass on SDS-PAGE for the *Capsicum* dehydrin may be explained by its higher mass based upon the deduced amino acid sequence.

We then compared the abundance of dehydrins in different organs under unstressed and stressed conditions. Immunoblot analysis revealed that the *Capsicum* and *Lycopersicon* dehydrins were constitutively present in all organs examined (Fig. 6b). The highest level of the proteins was detected in stems and roots. In wild tomato mature leaves, the protein was barely detected, whereas in pepper it was detected at a higher level. The accumulation pattern of the proteins in response to abiotic stresses was slightly different. In pepper, the protein accumulated in response to cold, salt and drought treatment. Drought treatment induced the highest level of the dehydrin, whereas cold treatment was less effective. In wild tomato, only a slight increase in protein accumulation was observed under cold-stress conditions, whereas in drought-stressed plants an increase in protein amount was highest. Stress-induced accumulation of *Capsicum* and *Lycopersicon* dehydrins was most evident in stems.

Based on the immunoblot analysis, we performed the tissue localization of DHN24 homologs in unstressed and drought-stressed plants. In mature pepper and wild tomato leaves of unstressed plants, the dehydrins were detected only in phloem (Fig. 7a, e). In stems and roots, the labeling was also detected in some cells of the phloem, whereas no labeling was observed in xylem, cortex and epidermis (Fig. 8a, d, i, k). In drought-stressed leaves of pepper and wild tomato, we observed an apparent increase in labeling intensity in most of the phloem cells (Fig. 7b–d, f). In some sections of wild tomato leaves, weaker labeling was also detected in stomatal guard cells (Fig. 7d). We could not detect the dehydrins in mesophyll and other epidermal cells. In drought-stressed stems, strong labeling was observed throughout the phloem in both species (Fig. 8b, c, e, f). In drought-stressed roots of pepper and wild tomato, fluorescent signal was also found in phloem cells (Fig. 8j, l). Sections incubated with preimmune antibodies were devoid of labeling (Figs. 7g, h, 8g, h, m, n).

Further experiments revealed that the acidic dehydrins were localized primarily to SEs and CCs of unstressed stems and roots (Fig. 9). Immunogold microscopy localized them to the cytosol and nuclei (Fig. 10b, d, g, k), parietal cytoplasm adjoining the cell wall of mature SEs (Fig. 10e), the lumen coincident with P-protein filaments (Fig. 10f, l) and in lower amounts in sieve-area pores of SEs (Fig. 10h). No labeling was obtained with preimmune antibodies (Fig. 10i, j).

Discussion

The role of acidic SK_3 dehydrins in the Solanaceae is not yet known. Although other studies have reported that the overexpression of acidic SK_n dehydrins from different species leads to improved tolerance to abiotic stresses in transgenic strawberries (Houde et al. 2004), *Arabidopsis* (Peng et al. 2008; Ochoa-Alfaro et al. 2012) and banana (Shekhawat et al. 2011), there is still limited information available about their precise tissue, cellular and intracellular locations. Identification of the tissues and cells in which the dehydrins accumulate is required to elucidate their potential or actual functions. Here, we report a detailed analysis of the tissue, cellular and subcellular localization of DHN24 and its homologous equivalents in unstressed and stressed plants of the Solanaceae family. We showed that DHN24 was specifically localized to the phloem cells of all organs examined under unstressed conditions (Fig. 1a, c, e, i). Further, our studies revealed that DHN24 was primarily detected in CCs and SEs of stems and roots (Fig. 3a, b, d). The SE/CC localization of DHN24 is clearly distinct from that of other acidic SK_n dehydrins from *Arabidopsis.* For example, ERD14 (SK_2) and LTI29 (SK_3) have been shown to be found in the root tip, vascular tissues and cells surrounding vascular tissues of unstressed roots (Nylander et al. 2001). In unstressed stems, ERD14 and LTI29 are localized to cortex, xylem, phloem and bordering parenchymal cells. Another member of this subclass, the DHN-COG from *Pisum sativum* (Robertson and Chandler 1994) is also present under normal growth conditions, but it is not known in which cell types the protein accumulates.

Under cold treatment, DHN24 accumulated in most cells of the phloem in roots, stems and leaves (Figs. 1b, d, f, j, k, 3c). Weaker labeling was sometimes detected in xylem parenchyma cells of stems (Fig. 1g). *Dhn24* mRNA was also abundantly present in phloem cells, which is consistent with the presence of the protein (Fig. 2a, b). In contrast, EDR14 and LTI29 exhibit the same pattern of

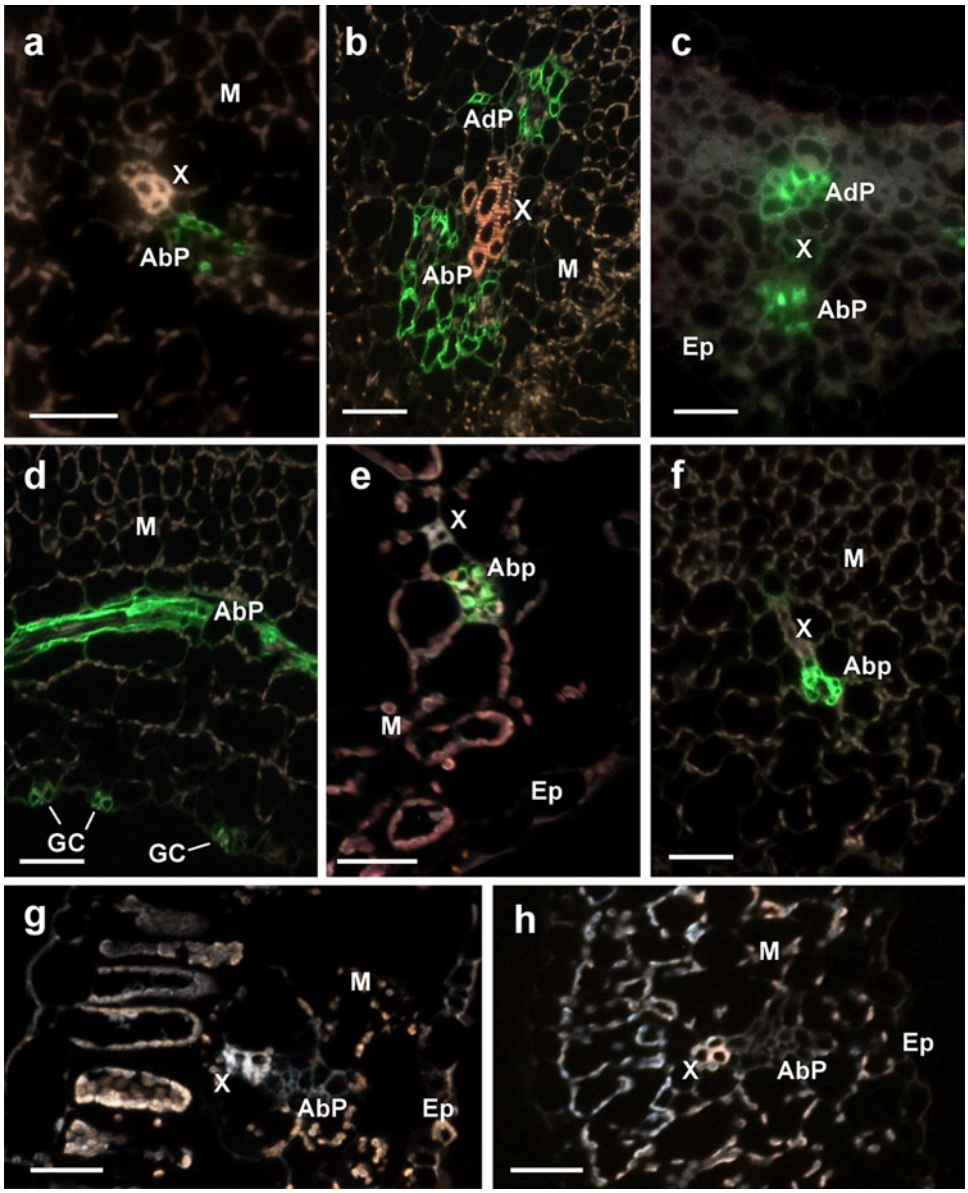

Fig. 7 Immunofluorescence localization of DHN24 homologs in leaves of *C. annuum and L. chilense.* Sections were incubated with anti-DHN24 polyclonal antibodies and labeled with secondary antibody conjugated to green fluorescent Alexa Fluor 488 dye. **a** Unstressed mature leaf (*L. chilense*). **b** Drought-stressed mature leaf (*L. chilense*). **c** Drought-stressed young leaf (*L. chilense*). **d** Section of drought-stressed mature leaf showing weaker labeling in stomata guard cells (*L. chilense*). **e** Unstressed mature leaf (*C.annuum*). **f** Drought-stressed mature leaf *(C. annuum)*. Sections of drought-stressed mature leaves of *L. chilense* (**g**) and *C. annuum* (**h**) treated with preimmune antibodies. *AbP* abaxial phloem, *AdP* adaxial phloem, *Co* cortex, *Ep* epidermis, *GC* guard cells, *M* mesophyll, *P* phloem, *X* xylem. *Bars* 25 μm

localization in cold-stressed stems as in unstressed stems (Nylander et al. 2001). In cold-treated leaves, EDR14 and LTI29 accumulate heavily in mesophyll cells, bundle sheath cells and vascular tissues. They are also found in guard cells. Another acidic SK_3 dehydrin from wheat WCOR410 is preferentially found in the perivascular region of crown, stem and root sections (Danyluk et al. 1998). The above data indicate that distinct regulatory mechanisms controlling tissue- and cell-specific expression exists among members of this subclass, which seems to be species-specific. Since DHN24 exhibits 84 and 89 % amino acid identity with *Capsicum* and *Lycopersicon* dehydrins, respectively, we were interested in determining whether the homologous dehydrins in the Solanaceae share similar properties. We found that the *Capsicum* and *Lycopersicon* dehydrins were also constitutively expressed, and their highest accumulation occurred in stems and roots (Fig. 6b). In response to abiotic stresses, the protein level was upregulated mainly by drought stress, although other stresses induced their accumulation. The pepper transcript has also been elevated by drought stress (Chung et al. 2003), but little and no accumulation occurs in response to salt and cold treatment. Similarly, the wild tomato transcript is also drought-inducible (Chen et al. 1993), which is consistent with our immunoblot analysis. The pattern of the stress-induced accumulation of *Capsicum* and *Lycopersicon* dehydrins is somewhat different from that of DHN24 that is mainly upregulated by cold treatment (Rorat et al. 2006). These results indicate that homologous acidic dehydrins of SK_3 type are constantly present in plant organs of

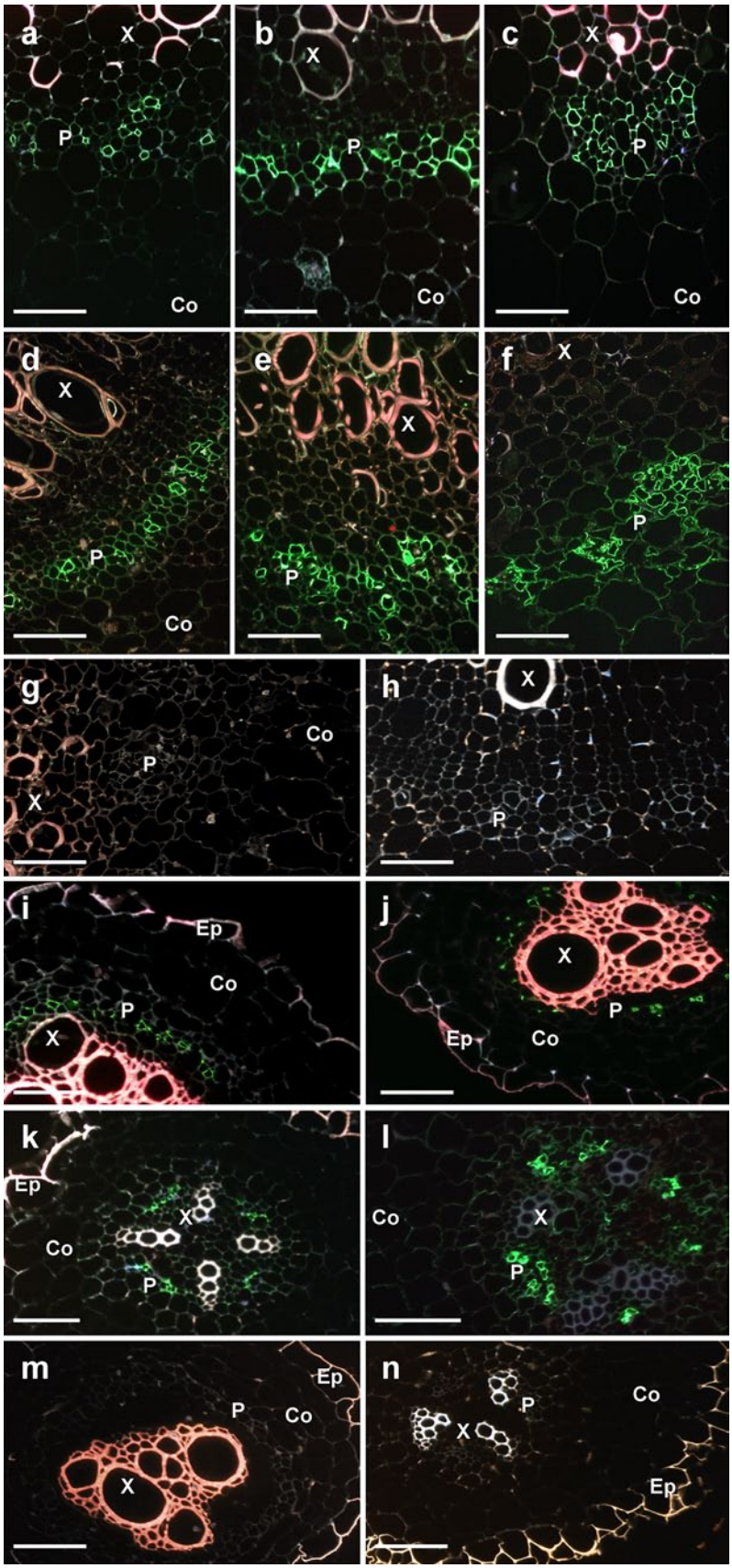

Fig. 8 Immunofluorescence localization of DHN24 homologs in stems and roots of *C. annuum and L. chilense.* Sections were incubated with anti-DHN24 polyclonal antibodies and labeled with secondary antibody conjugated to green fluorescent Alexa Fluor 488 dye. **a** Unstressed stem (*L. chilense*). **b**, **c** Drought-stressed stem (*L. chilense*). **d** Unstressed stem (*C. annuum*). **e**, **f** Drought-stressed stem (*C. annuum*). Sections of drought-stressed stems of *C. annuum* (**g**) and *L. chilense* (**h**) treated with preimmune antibodies. **i** Unstressed root (*L. chilense*). **j** Drought-stressed root (*L. chilense*). **k** Unstressed root (*C. annuum*). **l** Drought-stressed root (*C. annuum*). Sections of drought-stressed roots of *L. chilense* (**m**) and *C. annuum* (**n**) treated with preimmune antibodies. *Co* cortex, *Ep* epidermis, *P* phloem, *GC* guard cell, *X* xylem. *Bars* 25 μm

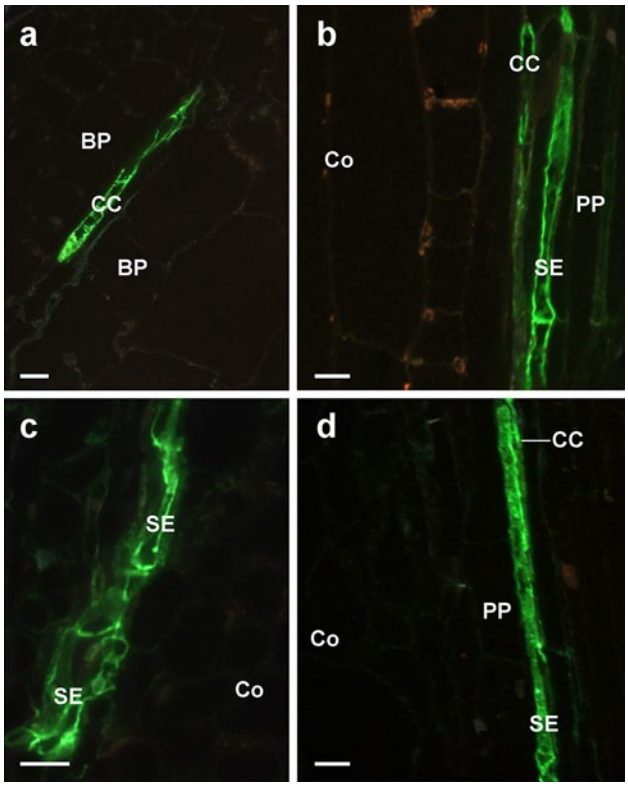

Fig. 9 Localization of DHN24 homologs to SEs and CCs of unstressed *L. chilense* and *C. annuum* plants. Stem and root longitudinal sections were incubated with anti-DHN24 polyclonal antibodies and labeled with secondary antibody conjugated to green fluorescent Alexa Fluor 488 dye. **a**, **b** Stem (*L. chilense*). **c** Stem (*C. annuum*). **d** Root (*C. annuum*). *BP* bordering parenchyma, *CC* companion cell, *Co* cortex, *PP* phloem parenchyma, *SE* sieve element. *Bars* 5 μm

the Solanaceae but can be upregulated differently possibly depending on the species, selective adaptation or their tolerance to abiotic stresses.

The *Lycopersicon* and *Capsicum* dehydrins were also found in SEs and CCs (Fig. 9) during normal growth and throughout the phloem in response to drought treatment (Figs. 7b, f; 8b, f). This indicates a high degree of conservation of these homologous acidic dehydrins at the tissue and cellular levels. A weaker labeling was sometimes observed in guard cells of drought-stressed *Lycopersicon* leaves (Fig. 7d), indicating that drought could induce the accumulation of the dehydrin or another closely related protein in these cells, but to a lower level than in the phloem. Since the tissue localization of acidic SK_n dehydrins in drought-stressed plants has not been reported in other plant systems, our studies provide valuable information about the site of accumulation of these proteins under water deficit.

The apparent constitutive expression of DHN24 and its homologs in SEs and CCs suggest a role in these highly specialized cells during normal growth. The phloem is the major route for delivering solutes from source to sink tissues and also plays a pivotal role in conveying signals via long-distance transport (Oparka and Turgeon 1999; Van Bel 2003; Lough and Lucas 2006). Many proteins indentified in SEs and CCs can be linked to stress and defense responses (Nolte and Koch 1993; Brugière et al. 1999; Hedley et al. 2000; Hause et al. 2003; Koiwai et al. 2004; Walz et al. 2004). To date, no reports have demonstrated the occurrence of acidic SK_n dehydrins in these cells. The constant presence of the Solanaceous dehydrins in SE/CC complexes might be beneficial to these important cell types, providing a protective environment in case of stress fluctuations. It might also be needed for effective and rapid induction of signal cascades at the commencement of stress exposure leading to the production of other defense molecules. Alternatively, the Solanaceous dehydrins might also play a role in the development of SEs since they appear to function in many development stages of SEs (Fig. 10e–h, l).

The appearance of DHN24 and its homologs in most of the phloem cells and in some other cells in response to cold and drought treatment may reflect the need for protection against cellular dehydration. Freezing temperatures and drought stress promote dehydration that causes cell shrinkage and concentration of cytoplasmic components, which can lead to protein aggregation and membrane dysfunction (Hoekstra et al. 2001; Guy 2003). It is believed that the protective function of dehydrins is mainly derived from their highly hydrophilic and unstructured nature (Mouillon et al. 2006; Hanin et al. 2011). Unfolded, hydrophilic regions allow dehydrins to form a large number of intermolecular hydrogen bonds and, therefore, stabilizing macromolecules in situations when water availability is limited (Bokor et al. 2005). Structural disorder also offers plasticity in partner binding and permits several functions for one protein (Tompa 2002; Tompa et al. 2005). The ability of one protein to perform numerous functions is known as moonlighting (Jeffery 1999), and this seems to be a feature of dehydrins. For example, in vitro studies have shown that ERD10 (SK_3) can bind calcium ions, water molecules, lipids and has chaperone and cryoprotective activities (Hara 2010; Hanin et al. 2011). Moonlighting functions of a protein can also be predicted by its diverse locations in the cell (Jeffery 1999). In accordance, DHN24 and its homologs were localized in different sites which suggests that they may serve different protective roles. They were abundantly found not only in the cytosol (Figs. 4b–d, 5a, 10d, k), but also in the nucleus (Figs. 4c, 5a, 10d, k), parietal cytoplasm adjoining the cell wall of mature SEs (Figs. 4j, 10e), the lumen coincident with P-protein filaments (Figs. 4k, 10f, l), the microsomal fraction (Fig. 5a) and close to the outer mitochondrial membranes (Fig. 4e). The cytosolic and nuclear localizations of the Solanaceous dehydrins are consistent with in silico predictions by WoLF PSORT (Horton

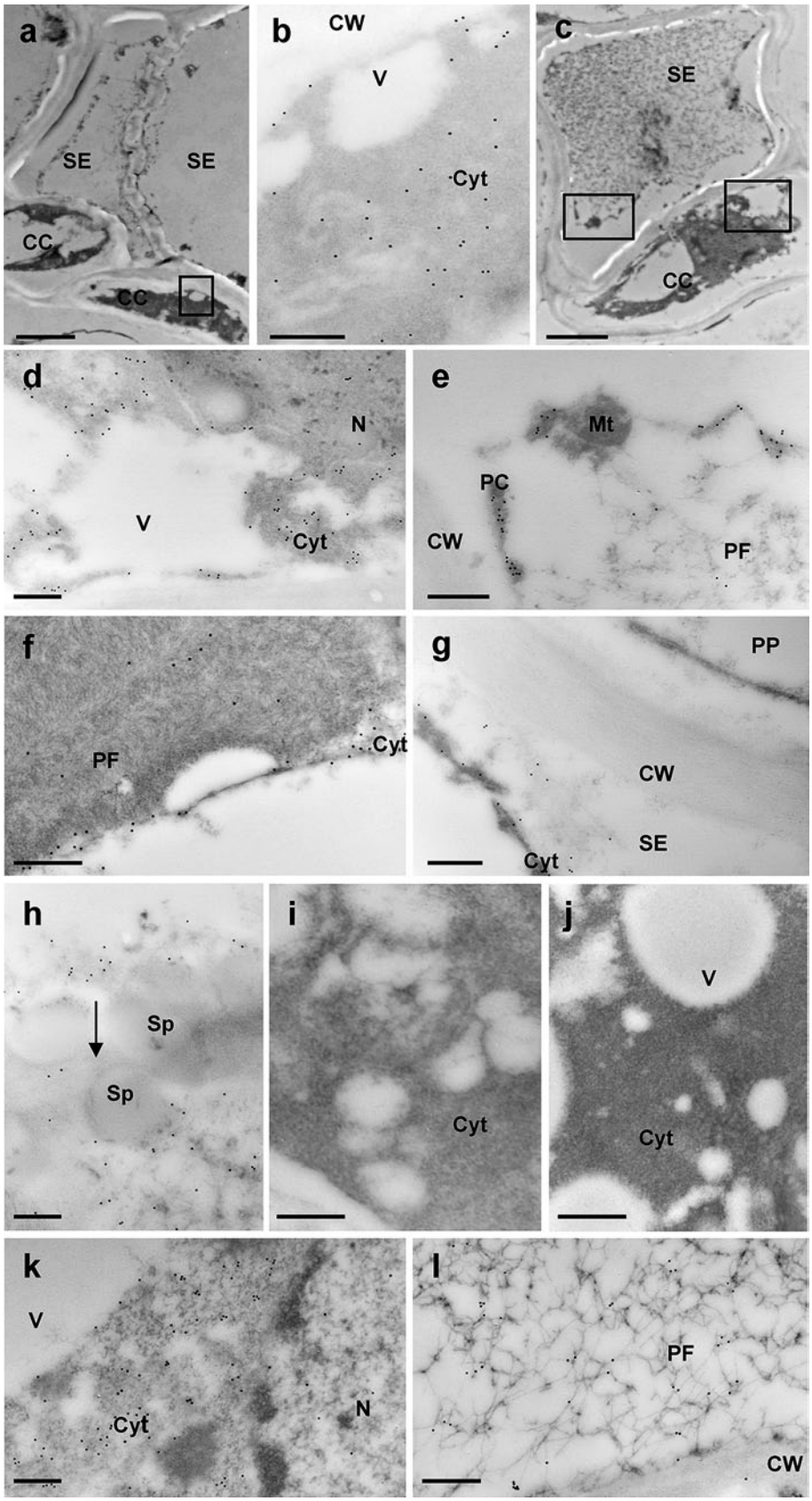
a
SE
SE
CC
CC
b
CW
V
Cyt
c
SE
CC
d
N
V
Cyt
e
Mt
PC
CW
PF
f
PF
Cyt
g
PP
CW
SE
Cyt
h
Sp
Sp
i
Cyt
j
V
Cyt
k
V
Cyt
N
l
PF
CW

◂**Fig. 10** Electron micrographs of unstressed and drought-stressed stem sections from *L. chilense* and *C. annuum*. Ultrathin sections of the phloem tissue of unstressed and drought-stressed stems were incubated with anti-DHN24 polyclonal antibodies or preimmune antibodies and labeled with secondary antibody conjugated to colloidal gold particles. **a** Phloem tissue showing the SE–CC complex. The *rectangle* in (**a**) is shown at higher magnification in (**b**). **b** High-magnification image from (**a**) showing localization of DHN24 homolog to the cytoplasm, unstressed stem (*L. chilense*). **c** Phloem tissue showing the SE–CC complex. The *rectangles* in (**c**) are shown at higher magnification in (**d**) and (**e**). **d** High-magnification image from (**c**) showing localization of DHN24 homolog to the cytoplasm and nucleus of CC, drought-stressed stem (*L. chilense*). **e** High-magnification image from (**c**) showing localization of DHN24 homolog to the parietal cytoplasm of mature SE, drought-stressed stem (*L. chilense*). **f** Localization of DHN24 homolog to the cytosol and lumen of differentiating SEs containing phloem protein (P-protein) filaments, unstressed stem (*L. chilense*). **g** Localization of DHN24 homolog to the cytosol of differentiating SEs, unstressed stem. (*L. chilense*). Note the absence of labeling in the cytosol of PP. **h** Weaker labeling of DHN24 homolog in sieve-area pores of the differentiating SEs. The arrow indicates the location of the sieve-area pores, unstressed stem (*L. chilense*). **i**, **j** Stem sections of *L. chilense* (**i**) and *C. annuum* (**j**) incubated with preimmune antibodies. **k** Localization of DHN24 homolog to the cytosol and nucleus, drought-stressed stem (*C. annuum*). **l** Localization of DHN24 homolog to the lumen of mature SE coincident with the presence of phloem protein (P-protein) filaments, unstressed stem (*C. annuum*). *CC* companion cell, *Cyt* cytosol, *CW* cell wall, *Mt* mitochondrion, *N* nucleus, *PF* P-protein filaments, *PP* phloem parenchyma, *SE* sieve element, *Sp* sieve plate, *V* vacuole. *Bars* 0.5 μm (**b**, **d**–**l**), 5 μm (**a**, **c**)

et al. 2007) and YLoc (Briesemeister et al. 2010) and with the previous reports that indicate the nuclear and cytosolic localization of dehydrins from Y_nSK_n (Goday et al. 1994; Godoy et al. 1994; Mehta et al. 2009) and K_n (Houde et al. 1995; Puhakainen et al. 2004) subclasses. However, the nuclear localization of other acidic SK_n dehydrins has not been unequivocally established. For example, WCOR410 (SK_3) accumulates in the vicinity of plasma membrane (Danyluk et al. 1998). *Arabidopsis* LITI29 (ERD10) is found in the cytoplasm (Puhakainen et al. 2004), although it has a putative nuclear localization signal (NLS) (Campos et al. 2006). Another acidic RcDhn5 (SK_2) from *Rhododendron catawbiense* has a putative NLS, but it is not known whether it can be imported into the nucleus (Peng et al. 2008). The amino acid sequence of DHN24 and its homologs does not contain a classical NLS required for nuclear import, but has the lysine-rich motif IKKKKKKG that partly resembles the NLS sequence (IKKKKKM) identified in the mouse type IV c-abl protein (Van Etten et al. 1989). Moreover, the Solanaceous dehydrins may be phosphorylated in planta (Szabala, unpublished data) and thus they might also be recruited to the nucleus on the basis of its phosphorylation state. It is believed that the nuclear import may also be regulated by phosphorylation (Nardozzi et al. 2010). It remains to be established how these proteins are imported into the nucleus and what protective role they may have in this compartment. The microsomal localization and detection close to the outer mitochondrial membranes are consistent with previous reports indicating that acidic SK_n dehydrins may have a role in protecting membranes from freeze-induced dehydration (Danyluk et al. 1998; Puhakainen et al. 2004). The presence of DHN24 and its homologs in the parietal cytoplasm and the lumen of mature SEs coincident with the presence of phloem protein (P-protein) filaments represents a new observation that has not been previously reported for dehydrins. SEs undergo a controlled disintegration process during their development, in which the nuclei, ribosomes, vacuolar membrane and cytoskeletal elements are lost, whereas P-proteins, modified mitochondria, plastids and parietal cytoplasm are retained. Since mature SEs are incapable of protein synthesis, their function depends on CCs from which many macromolecules are passed into SEs (Oparka and Turgeon 1999; Knoblauch and Oparka 2012). Identification of the dehydrin proteins in mature SEs suggests that they might be transported into SEs from CCs and constitute a network of proteins needed to maintain or protect enucleated SEs. The weaker localization of DHN24 and its homologs in sieve-area pores (Figs. 4i, 10h) further suggests that they might be translocated between neighboring SEs.

In summary, our study brings a substantial insight into the localization of Solanaceous acidic SK_3 dehydrins during optimal growth, and under cold and drought stress. The identification and characterization of the tissues, cells and intracellular compartments in which DHN24 and its homologs accumulate provide important information regarding their potential roles in the Solanaceae. The strongest accumulation of these proteins in phloem may be related to a function in preventing the region from harmful effect of dehydration imposed by abiotic stresses. Further studies will characterize the biochemical, protective and structural properties of DHN24.

Acknowledgments Prof. Zbigniew Miszalski (IPP, PAS, Cracow) is acknowledged for comments on the manuscript. Malgorzata Wasilewska-Gomulka is acknowledged for ultramicrotome work. This work was supported in part by the Ministry of Science and Higher Education, Grant No. PBZ/MNiSW-2/3/2006.

Conflict of interest The authors declare that they have no conflict of interest.

References

Alsheikh MK, Svensson JT, Randall SK (2005) Phosphorylation regulated ion-binding is a property shared by the acidic subclass dehydrins. Plant Cell Environ 28:1114–1122

Bartels D, Sunkar R (2005) Drought and salt tolerance in plants. Crit Rev Plant Sci 24:23–58

Baskin TI, Busby CH, Fowke LC, Sammut M, Gubler F (1992) Improvements in immunostaining samples embedded in

methacrylate: localization of microtubules and other antigens throughout developing organs in plants of diverse taxa. Planta 187:405–413

Bokor M, Csizmok V, Kovacs D, Banki P, Friedrich P, Tompa P, Tompa K (2005) NMR relaxation studies on the hydrate layer of intrinsically unstructured proteins. Biophys J 88:2030–2037

Borovskii GB, Stupnikova IV, Antipina AA, Downs CA, Voinikov VK (2000) Accumulation of dehydrin-like-proteins in the mitochondria of cold-treated plants. J Plant Physiol 156:797–800

Briesemeister S, Rahnenführer J, Kohlbacher O (2010) YLoc—an interpretable web server for predicting subcellular localization. Nucleic Acids Res 38:W497–W502

Brugière N, Dubois F, Limami AM, Lelandais M, Roux Y, Sangwan RS, Hirel B (1999) Glutamine synthetase in the phloem plays a major role in controlling proline production. Plant Cell 11:1995–2011

Campos F, Zamudio F, Covarrubias AA (2006) Two different late embryogenesis abundant proteins from *Arabidopsis thaliana* contain specific domains that inhibit *Escherichia coli* growth. Biochem Biophys Res Commun 342:406–413

Chen RD, Campeau N, Greer AF, Bellemare G, Tabaeizadeh Z (1993) Sequence of a novel abscisic acid- and drought-induced cDNA from wild tomato (*Lycopersicon chilense*). Plant Physiol 103:301

Chung F, Kim S-Y, Yi SY, Choi D (2003) *Capsicum annum* dehydrin, an osmotic-stress gene in hot paper plants. Mol Cells 15:327–332

Close TJ (1997) Dehydrins: a commonalty in the response of plants to dehydration and low temperature. Physiol Plant 100:291–296

Danyluk J, Houde M, Rassart E, Sarhan F (1994) Differential expression of a gene encoding an acidic dehydrin in chilling sensitive and freezing tolerant gramineae species. FEBS Lett 344:20–24

Danyluk J, Perron A, Houde M, Limin A, Fowler B, Benhamou N, Sarhan F (1998) Accumulation of an acidic dehydrin in the vicinity of the plasma membrane during cold acclimation of wheat. Plant Cell 10:623–638

Dykstra MJ, Reuss LE (2003) Biological electron microscopy: theory, techniques and troubleshooting, 2nd edn. Kluwer Acad/Plenum Publ, New York, pp 101–103

Egerton-Warburton LM, Balsamo RA, Close TJ (1997) Temporal accumulation and ultrastructural localization of dehydrins in *Zea mays*. Physiol Plant 101:545–555

Fudali S, Janakowski S, Sobczak M, Griesser M, Grundler FM, Golinowski W (2008) Two tomato alpha-expansins show distinct spatial and temporal expression patterns during development of nematode-induced syncytia. Physiol Plant 132:370–383

Goday A, Jensen AB, Culianez-Macia FA, Alba MM, Figueras M, Serratosa J, Torrent M, Pages M (1994) The maize abscisic acid-responsive protein Rab17 is located in the nucleus and interacts with nuclear localization signals. Plant Cell 6:351–360

Godoy JA, Lunar R, Torres-Schumann S, Moreno J, Rodrigo RM, Pintor-Toro JA (1994) Expression, tissue distribution and subcellular localization of dehydrin TAS14 in salt-stressed tomato plants. Plant Mol Biol 26:1921–1934

Guy CL (2003) Freezing tolerance of plants: current understanding and selected emerging concepts. Can J Bot 81:1216–1223

Hanin M, Brini F, Ebel C, Toda Y, Takeda S, Masmoudi K (2011) Plant dehydrins and stress tolerance: versatile proteins for complex mechanisms. Plant Signal Behav 6:1503–1509

Hara M (2010) The multifunctionality of dehydrins: an overview. Plant Signal Behav 5:503–508

Hara M, Terashima S, Fukaya T, Kuboi T (2003) Enhancement of cold tolerance and inhibition of lipid peroxidation by citrus dehydrin in transgenic tobacco. Planta 217:290–298

Hara M, Fujinaga M, Kuboi T (2004) Radical scavenging activity and oxidative modification of citrus dehydrin. Plant Physiol Biochem 42:657–662

Hara M, Kondo M, Kato T (2013) A KS-type dehydrin and its related domains reduce Cu-promoted radical generation and the histidine residues contribute to the radical-reducing activities. J Exp Bot 64:1615–1624

Hara M, Shinoda Y, Tanaka Y, Kuboi T (2009) DNA binding of citrus dehydrin promoted by zinc ion. Plant Cell Environ 32:532–541

Hause B, Hause G, Kutter C, Miersch O, Wasternack C (2003) Enzymes of jasmonate biosynthesis occur in tomato sieve elements. Plant Cell Physiol 44:643–648

Hedley PE, Maddison AL, Davidson D, Machray GC (2000) Differential expression of invertase genes in internal and external phloem tissues of potato (*Solanum tuberosum* L.). J Exp Bot 51: 817–821

Heyen BJ, Alsheikh MK, Smith EA, Torvik CF, Seals DF, Randall SK (2002) The calcium-binding activity of a vacuole-associated, dehydrin-like protein is regulated by phosphorylation. Plant Physiol 130:675–687

Hoekstra FA, Golovina EA, Buitnik J (2001) Mechanism of plant desiccation tolerance. Trends Plant Sci 6:431–438

Horton P, Park KJ, Obayashi T, Fujita N, Harada H, Adams-Collier CJ, Nakai K (2007) WoLF PSORT: protein localization predictor. Nucleic Acid Res 35:W585–W587

Houde M, Daniel C, Lachapelle M, Allard F, Laliberte S, Sarhan F (1995) Immunolocalization of freezing-tolerance-associated proteins in the cytoplasm and nucleoplasm of wheat crown tissues. Plant J 8:583–593

Houde M, Dallaire S, N'Dong D, Sarhan F (2004) Overexpression of the acidic dehydrin WCOR410 improves freezing tolerance in transgenic strawberry leaves. Plant Biotechnol J 2:381–387

Jeffery CJ (1999) Moonlighting proteins. Trends Biochem Sci 24:8–11

Knoblauch M, Oparka K (2012) The structure of the phloem—still more questions than answers. Plant J 70:147–156

Koag MC, Fenton RD, Wilkens S, Close TJ (2003) The binding of maize DHN1 to lipid vesicles. Gain of structure and lipid specificity. Plant Physiol 131:309–316

Koag MC, Wilkens S, Fenton RD, Resnik J, Vo E, Close TJ (2009) The K-segment of maize DHN1 mediates binding to anionic phospholipid vesicles and concomitant structural changes. Plant Physiol 150:1503–1514

Koiwai H, Nakaminami K, Seo M, Mitsuhashi W, Toyomasu T, Koshiba T (2004) Tissue-specific localization of an abscisic acid biosynthetic enzyme, AAO3, in Arabidopsis. Plant Physiol 134:1697–1707

Kovacs D, Kalmar E, Torok Z, Tompa P (2008) Chaperone activity of ERD10 and ERD14, two disordered stress-related plant proteins. Plant Physiol 147:381–390

Lough TJ, Lucas WJ (2006) Integrative plant biology: role of phloem long-distance macromolecular trafficking. Annu Rev Plant Biol 57:203–232

Mahajan S, Tuteja N (2005) Cold, salinity and drought stresses: an overview. Arch Biochem Biophys 444:139–158

Mehta PA, Rebala KC, Venkataraman G, Parida A (2009) A diurnally regulated dehydrin from *Avicennia marina* that shows nucleocytoplasmic localization and is phosphorylated by casein kinase II in vitro. Plant Physiol Biochem 47:701–709

Millar AH, Liddell A, Leaver CJ (2007) Isolation and subfractionation of mitochondria from plants. In: Pon LA, Schon EA (eds) Methods in cell biology, 2nd edn. Elsevier Inc, New York, pp 65–90

Mouillon JM, Gustafsson P, Harryson P (2006) Structural investigation of disordered stress proteins. Comparison of full-length dehydrins with isolated peptides of their conserved segments. Plant Physiol 141:638–650

Nardozzi JD, Lott K, Cingolani G (2010) Phosphorylation meets nuclear import: a review. Cell Commun Signal 8:32

Nolte KD, Koch KE (1993) Companion-cell specific localization of sucrose synthase in zones of phloem loading and unloading. Plant Physiol 101:899–905

Nylander M, Svensson J, Palva ET, Welin BV (2001) Stress-induced accumulation and tissue-specific localization of dehydrins in *Arabidopsis thaliana*. Plant Mol Biol 45:263–279

Ochoa-Alfaro AE, Rodríguez-Kessler M, Pérez-Morales MB, Delgado-Sánchez P, Cuevas-Velazquez CL, Gómez-Anduro G, Jiménez-Bremont JF (2012) Functional characterization of an acidic SK_3 dehydrin isolated from an *Opuntia streptacantha* cDNA library. Planta 235:565–578

Oparka KJ, Turgeon R (1999) Sieve elements and companion cells—traffic control centers of the phloem. Plant Cell 11:739–750

Peng Y, Reyes JL, Wei H, Yang Y, Karlson D, Covarrubias AA, Krebs SL, Fessehaie A, Arora R (2008) RcDhn5, a cold acclimation-responsive dehydrin from *Rhododendron catawbiense* rescues enzyme activity from dehydration effects in vitro and enhances freezing tolerance in RcDhn5-overexpressing *Arabidopsis* plants. Physiol Plant 134:583–597

Puhakainen T, Hess MV, Makela P, Svenson J, Heino P, Palva ET (2004) Overexpression of multiple dehydrin genes enhances tolerance to freezing stress in *Arabidopsis*. Plant Mol Biol 54:743–753

Robertson M, Chandler PM (1994) A dehydrin cognate protein from pea (*Pisum sativum L.*) with an atypical pattern of expression. Plant Mol Biol 26:805–816

Rorat T (2006) Plant dehydrins—tissue location, structure and function. Cell Mol Biol Lett 11:536–556

Rorat T, Szabala BM, Grygorowicz WJ, Wojtowicz B, Yin Z, Rey P (2006) Expression of SK_3-type dehydrin in transporting organs is associated with cold acclimation in *Solanum* species. Planta 224:205–221

Shekhawat UK, Srinivas L, Ganapathi TR (2011) MusaDHN-1, a novel multiple stress-inducible SK_3-type dehydrin gene, contributes affirmatively to drought- and salt-stress tolerance in banana. Planta 234:915–932

Svensson J, Palva ET, Welin B (2000) Purification of recombinant *Arabidopsis thaliana* dehydrins by metal ion affinity chromatography. Protein Expr Purif 20:169–178

Tompa P (2002) Intrinsically unstructured proteins. Trends Biochem Sci 27:527–533

Tompa P, Szasz C, Buday L (2005) Structural disorder throws new light on moonlighting. Trends Biochem Sci 30:484–489

Van Bel AJE (2003) The phloem, a miracle of ingenuity. Plant Cell Environ 26:125–149

Van Bel AJE, Ehlers K, Knoblauch M (2002) Sieve elements caught in the act. Trends Plant Sci 7:126–132

Van Etten RA, Jackson P, Baltimore D (1989) The mouse type IV c-abl gene product is a nuclear protein, and activation of transforming ability is associated with cytoplasmic localization. Cell 58:669–678

Van Wijk K, Peltier JB, Giacomelli L (2007) Isolation of chloroplast proteins from *Arabidopsis thaliana* for proteome analysis. In: Thiellement H, Zivy M, Damerval C, Mechin V (eds) Plant proteomics: methods and protocols. Humana Press, New Jersey, pp 43–48

Walz C, Giavalisco P, Schad M, Juenger M, Klose J, Kehr J (2004) Proteomics of curcurbit phloem exudate reveals a network of defence proteins. Phytochemistry 65:1795–1804